JOURNAL OF GUIDANCE, CONTROL, AND DYNAMICS
Vol. 27, No. 4, July–August 2004

Flight Dynamics of the Boomerang, Part 2: Effects of Initial Conditions and Geometrical Configuration

Goro Beppu* and Hiroaki Ishikawa†
Tokai University, Hiratsuka 259-1292, Japan
Akira Azuma‡
University of Tokyo, Kawasaki 212-0021, Japan
and
Kunio Yasuda§
Nihon University, Funabashi 274-8501, Japan

In Part 1, equations of motion for boomerang flight dynamics were presented in strictly nonlinear form and solved numerically for a typical returning boomerang. The solution shows that the motion consists of both long- and short-period oscillations. These oscillations were found to be the result of the aerodynamically asymmetric moment and the gyro effect of the spinning motion with high advance ratio. When either the initial conditions at takeoff or the geometrical characteristics of the boomerang were varied, various flight paths and flight performances were obtained, some of which are compared with experimental results. The detailed mechanisms of the returning path, tennis racket effect on the flight stability, and ways of throwing a boomerang to avoid dangerous flight path are presented.

Nomenclature

$\boldsymbol{J}$	=	inertial tensor, $(I_x, I_y, I_z, J_{xy}, J_{xz})^T$
$\boldsymbol{J}_j$	=	moment and product of inertia of jth blade, $(I_{\xi,j}, I_{\eta,j}, I_{\varsigma,j}, J_{\xi\eta,j} J_{\xi\varsigma,j})^T$
$\boldsymbol{M}^1$	=	inertial moment in body frame, $(M_x^I, M_y^I, M_z^I)^T$
m	=	mass of boomerang
$\boldsymbol{R}$	=	position vector of the origin of body frame in inertial frame, $(X_I, Y_I, Z_I)^T$
R	=	reference radius
$\boldsymbol{r}$	=	any position vector in body frame, $(x, y, z)^T$
t	=	time
$\boldsymbol{U}$	=	translational velocity of the origin of body frame and nonslipping frame expressed in inertial frame, $\dot{\boldsymbol{R}}$ equal to $(\dot{X}, \dot{Y}, \dot{Z})^T$
α	=	angle of attack of blade element
α_{stall}	=	stalling angle of attack
β_j	=	coning angle, rotation about x_2 axis
γ	=	folding angle or joint angle of two blades, $\Lambda_2 - \Lambda_1$
$\Delta\theta_t$	=	blade twist, positive for washin
$\Delta\Lambda$	=	differential angle, $\pi - \gamma$
δ	=	differential angle showing tennis racket effect
θ	=	feathering angle, rotation about Y_1 axis
θ_j	=	pitch angle, rotation about y_3 axis
Λ_j	=	sweep angle, rotation about z_1 axis
ρ	=	air density
Φ	=	rolling angle or bank angle of non-spinning axis, rotation about X_B axis
$\boldsymbol{\omega}$	=	angular velocity, $(p, q, r)^T$

Subscripts

j	=	jth state
0	=	initial state

Superscripts

A	=	aerodynamic component
G	=	gravitational component
I	=	inertial component

Introduction

IN Part I, the theoretical analysis and numerical computations on the flight dynamics of a typical returning boomerang were presented. In this Part II, effects of initial conditions and geometrical configurations will be discussed in comparison with those of the reference boomerang.

Effects of Initial Conditions on the Flight Performance

Initial Speed

Changing the launching speed by ±5 m/s from the reference speed of $U_0 = 25$ m/s used in Ref. 1 produces two different flight paths, as shown in Figs. 1a–1f. When the initial flight speed U_0 is reduced from 25 to 20 m/s, the excursion shown by a dashed curve with cross symbols has a smaller radius of curvature than that of the reference excursion shown by a solid curve, and the boomerang lands at about the 35th rotation, 3 m short of reaching the initial takeoff point. At a higher launching speed, $U_0 = 30$ m/s, the excursion shown by a dot–dash curve with square symbols has a larger radius of curvature and obtains higher altitude Z than that of the reference flight path. However, the boomerang falls or lands at about the 35th rotation after overshooting the initial takeoff point by about 2 m. Because of higher initial speed, the kinetic energy and the total energy are larger than that of the reference excursion and thus the flight distance increases by having larger radii of curvature (caused by the larger centrifugal force) and by maintaining higher altitude (caused by larger lift) than those of the reference excursion. Changes in other quantities such as angular velocity and Euler's angles did not appreciably alter the general flight behavior.

Initial Rolling Angle

When the initial rolling angle is changed ±10 deg from the reference angle of $\Phi_0 = 70$ deg, two different flight paths are obtained, as shown in Figs. 2a–2f. When the initial rolling angle is reduced

Received 13 January 2003; revision received 17 July 2003; accepted for publication 29 September 2003.

*Professor, Department of Aeronautics and Astronautics.
†Graduate Student, Department of Aeronautics and Astronautics.
‡Professor Emeritus, 37-3 Miyako-cho, Saiwai-ku. Senior Member AIAA.
§Associate Professor, Department of Aerospace Engineering. Senior Member AIAA.

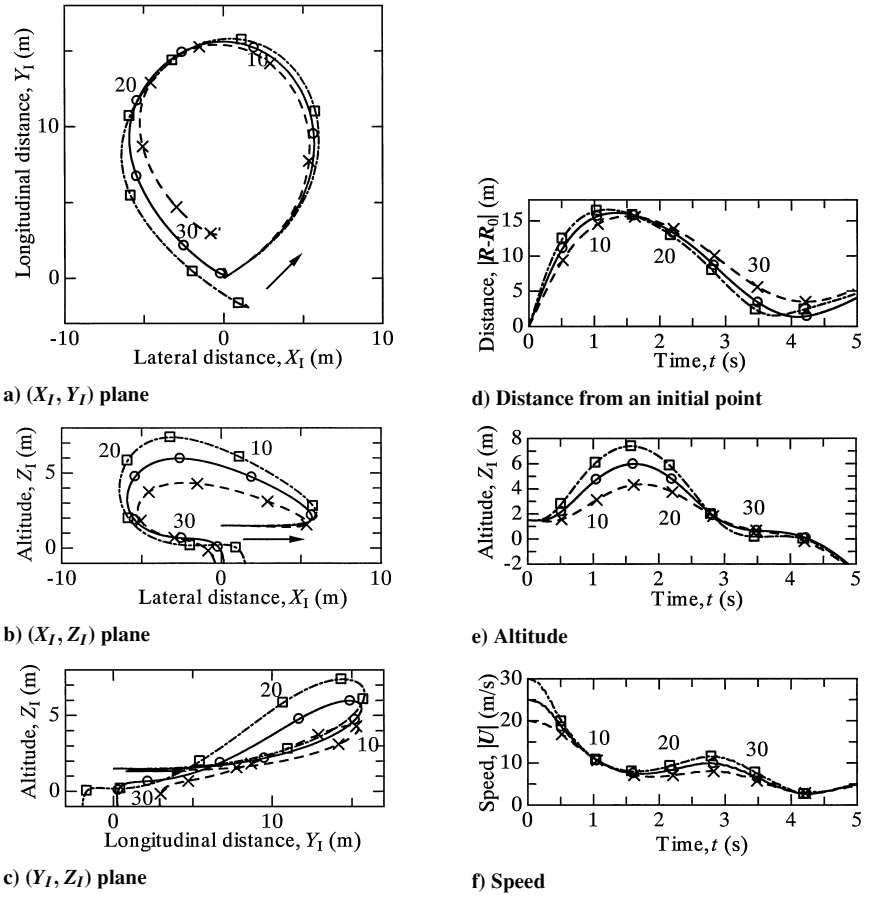

Fig. 1 Effect of the initial speed U_0 on the excursion flight path and speed; $r_0 = 10$ Hz and $\Phi_0 = 70$ deg: –×–, $U_0 = 20$ m/s; —○—, $U_0 = 25$ m/s; and – -□- –, $U_0 = 30$ m/s.

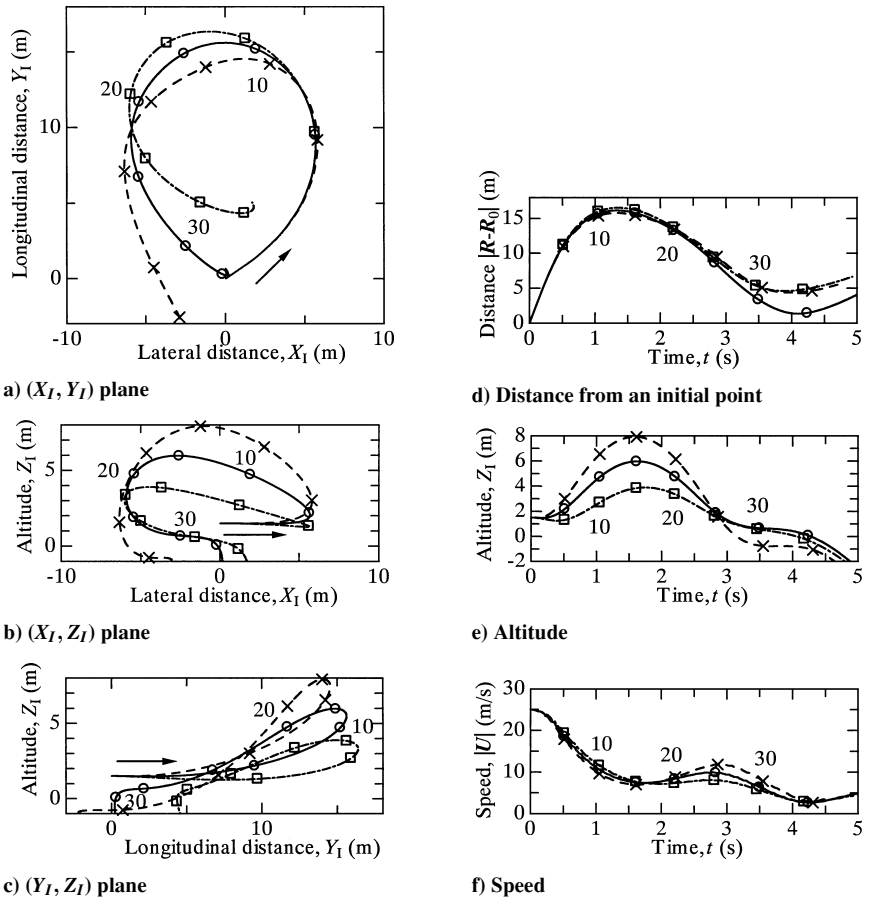

Fig. 2 Effect of the initial rolling angle Φ_0 on the excursion flight path and speed; $U_0 = 25$ m/s and $r_0 = 10$ Hz: –×–, $\Phi_0 = 60$ deg; —○—, $\Phi_0 = 70$ deg; and – -□- –, $\Phi_0 = 80$ deg.

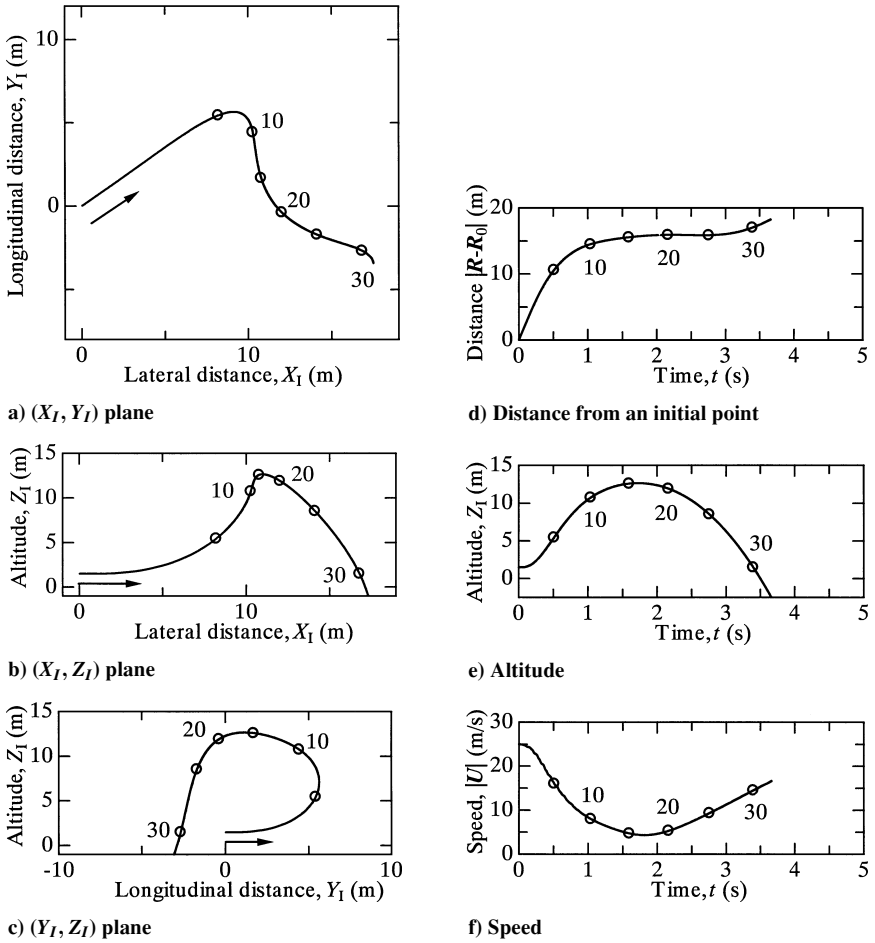

Fig. 3 Excursion flight path of boomerang thrown with the initial rolling angle $\Phi_0 = 0$ deg; $U_0 = 25$ m/s and $r_0 = 10$ Hz.

(increased) from 70 to 60 deg (80 deg), the calculated excursion shown by a dashed curve (dot-dashed curve) is shorter (longer) in maximum distance $|\boldsymbol{R} - \boldsymbol{R}_0|_{\max}$. The same computation results in a higher (lower) altitude Z than that of the reference flight path as shown by a solid curve because of the larger (smaller) upward lift imparted initially. Then, in the latter half of the flight, this results in much higher (lower) speed than the reference case and the radius of curvature becomes smaller (greater). In the case of $\Phi_0 = 60$ deg, the boomerang descends more rapidly and lands sooner than in the other two cases. On the other hand, in the case of $\Phi_0 = 80$ deg, the boomerang is seen to have a lower rate of descent in a long duration. In all of the flights, the thrower located at the launching point cannot catch the returning boomerang because the point of landing is nearly 5 m away.

It is usually not advisable to throw the boomerang with very small rolling angle, such as flat or parallel to the ground, $\Phi_0 = 0$ deg. In this case, as shown in Figs. 3a–3f, the boomerang makes a right turn (clockwise), unlike the left turn (counter-clockwise) of the preceding results, rises sharply, and then, after having reached the highest altitude, which is more than 10 m, it descends steeply and plummets to the ground at near the 30th rotation with a flight speed of more than 15 m/s. The impact may damage the boomerang. Because of the steep climb in the first chronological block, the flight speed decelerates sharply. However, the spin rate remains constant throughout the flight. When the boomerang has a forward velocity, the positive pitching moment is generated on the apparent disk (as shown in Fig. 9c in Ref. 1). As a result (principally from the gyroprecession), the apparent disk of the boomerang has negative roll angle (positive bank angle), which is because the apparent disk initially has the zero roll angle in this case. This roll angle causes the rightward tilt of the normal force acting on the apparent disk and the right turn for the boomerang, although in the reference case, the boomerang turns in the left direction.

Initial Spin Rate

When the initial spin rate is changed from the reference speed of $r_0 = 10$ Hz (62.8 rad/s) by ± 2 Hz, two different flight paths are obtained, as shown in Figs. 4a–4f. When the spin rate is reduced to $r_0 = 8$ Hz, the turning radius becomes small, and the boomerang lands about 5 m away from the takeoff point. On the other hand, in the flight initiated with a spin rate of $r_0 = 12$ Hz, the turning radius becomes large, and at the final phase of the flight, the boomerang makes similar turning flight, accompanied by a higher vertical excursion before it drops to the ground. The larger turning radius for a spin rate of $r_0 = 12$ Hz results for the following reason: A higher spin rate enables the boomerang to climb to a higher altitude; thereby, in descending flight, a higher flight speed and a larger turn radius are obtained. In either flight, the maximum distance in the forward direction $|Y_I|_{\max}$ and, thus, the maximum resultant distance $|\boldsymbol{R} - \boldsymbol{R}_0|_{\max}$ are almost unchanged from those of the reference flight. In either case, the boomerang plummets to the ground at high speed differently from the case of the reference rate of spin. A higher spin rate enables the boomerang to climb to a higher altitude, thereby accelerating to a higher speed in descent causing a larger turning radius, and hence the overshoot in a manner quite similar to that shown in Fig. 1.

As shown in Figs. 5a–5c, in the case of the reduced initial-spin-rate, the amplitude of the short-period oscillation increases appreciably between the 10th and 20th rotations in the descending flight and the spin-rate decreases monotonically. On the other hand, as shown in Figs. 5d–5f, in the case of the increased initial spin rate, the amplitude of the short-period oscillation in descending flight decreases because of the tennis-racket or centrifugal force effect

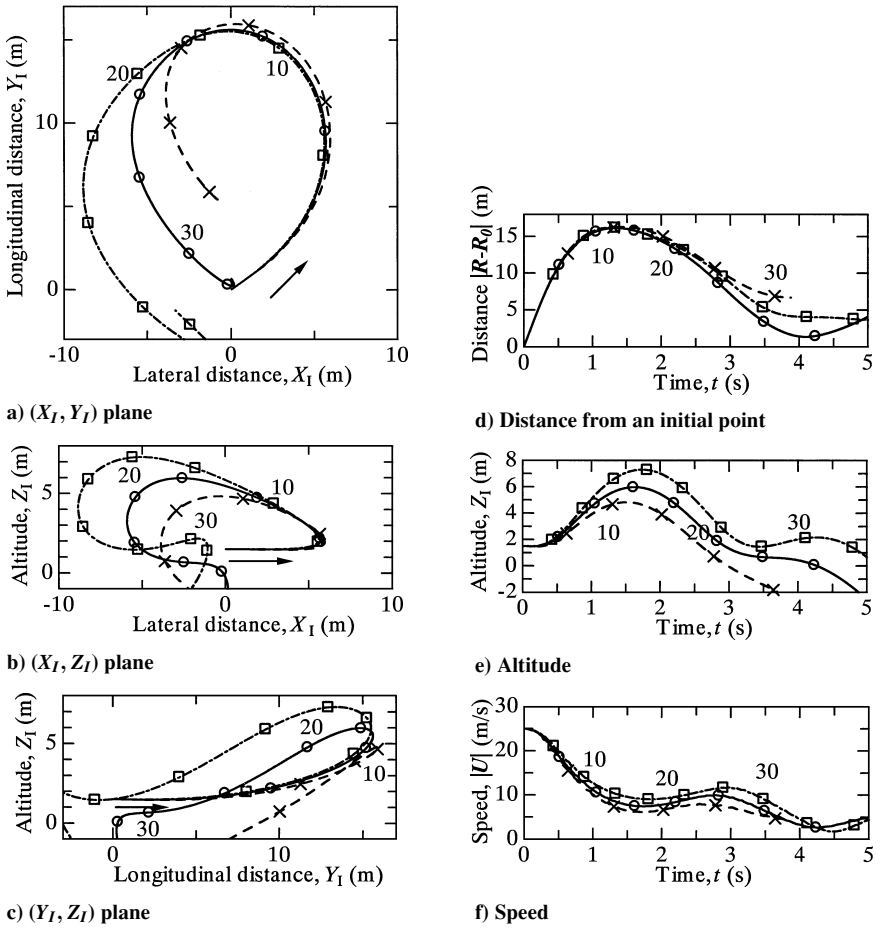

Fig. 4 Effect of the initial spin rate r_0 on the excursion and time history; $U_0 = 25$ m/s and $\Phi_0 = 70$ deg: –×–, $r_0 = 8$ Hz; —⊖—, $r_0 = 10$ Hz; and – -□- –, $r_0 = 12$ Hz.

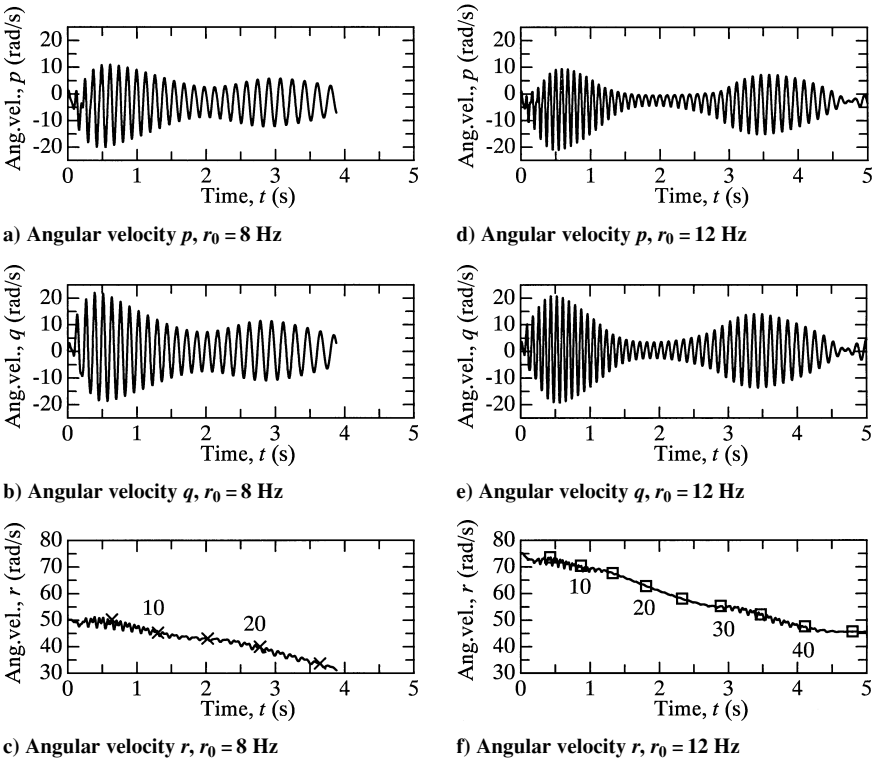

Fig. 5 Time history of the flight of initial spin rates $r_0 = 8$ and 12 Hz; $U_0 = 25$ m/s and $\Phi_0 = 70$ deg.

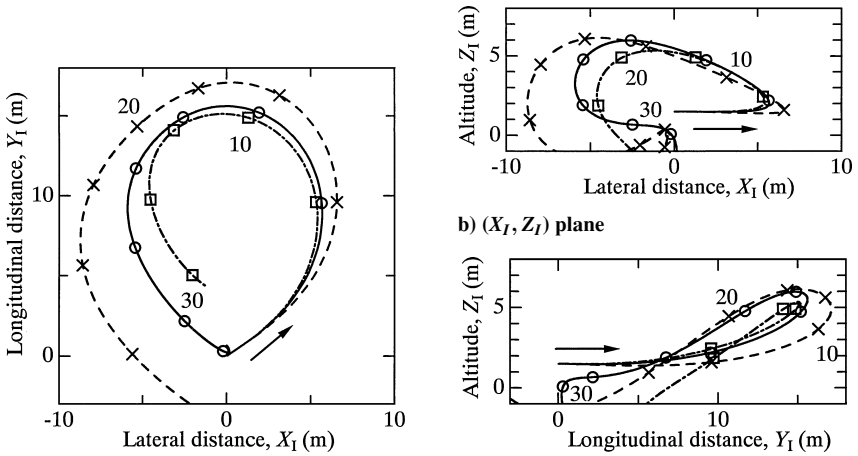

a) (X_I, Y_I) plane

b) (X_I, Z_I) plane

c) (Y_I, Z_I) plane

Fig. 6 Effect of the pitch angle θ_j on the excursion; $U_0 = 25$ m/s, $r_0 = 10$ Hz, and $\Phi_0 = 70$ deg: –×–, $\theta_j = -1.0$ deg; —○—, $\theta_j = 0.0$ deg; and – -□- –, $\theta_j = +1.0$ deg.

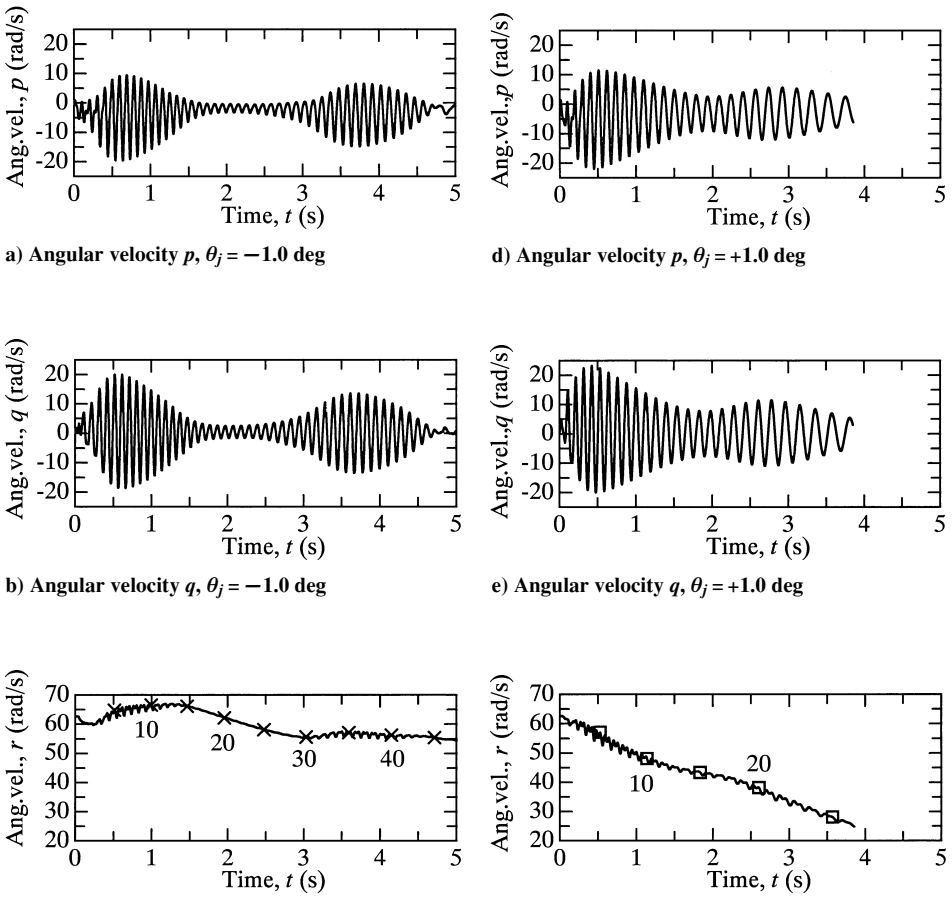

a) Angular velocity p, $\theta_j = -1.0$ deg

b) Angular velocity q, $\theta_j = -1.0$ deg

c) Angular velocity r, $\theta_j = -1.0$ deg

d) Angular velocity p, $\theta_j = +1.0$ deg

e) Angular velocity q, $\theta_j = +1.0$ deg

f) Angular velocity r, $\theta_j = +1.0$ deg

Fig. 7 Time history of angular velocity of pitch angle $\theta_j = -1.0$ and +1.0 deg; $U_0 = 25$ m/s, $r_0 = 10$ Hz, and $\Phi_0 = 70$ deg.

caused by the spin rate over the entire flight range being larger than in the other two cases.

Effects of Geometrical Configuration on Flight Performance

Pitch Angle

As the blade pitch angle increases from $\theta_j = -1.0$ through $\theta_j = 0$ deg of the reference boomerang to $\theta_j = +1.0$ deg, the radius of curvature, the maximum distance from the takeoff point, and the maximum altitude and the flight duration decrease as shown in Figs. 6a–6c. As shown in Figs. 7a–7c, in the case of lower pitch angle $\theta_j = -1.0$ deg, the negative pitch produces an increase in spin rate and in the kinetic energy of spinning motion caused by autorotation. Thus, the amplitude of short-period oscillation decreases. As shown in Fig. 8a, this is clearly demonstrated by the fact that the driving force or the driving torque (negative torque) increases as the pitch angle decreases. At high pitch angle $\theta_j = +1.0$ deg, on the other hand, the spin rate decreases markedly as shown in Fig. 7f because, as shown in Fig. 8b, no autorotational effect arises. Accompanying the decrease of spin rate, the short-period oscillation can be observed in every chronological block or for the entire flight duration as seen from Figs. 7d and 7e.

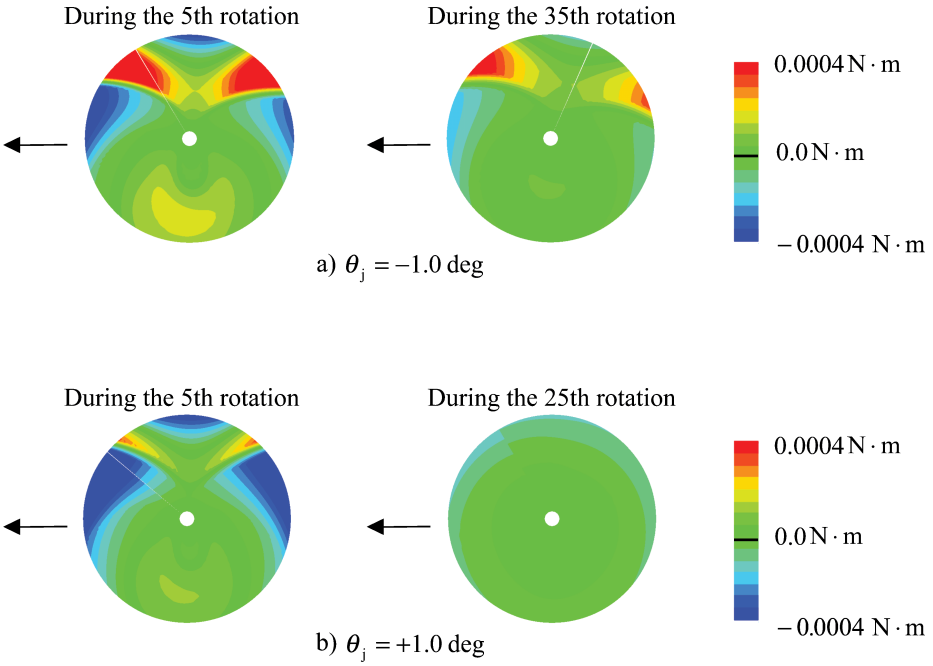

Fig. 8 Changes in distribution of driving torque.

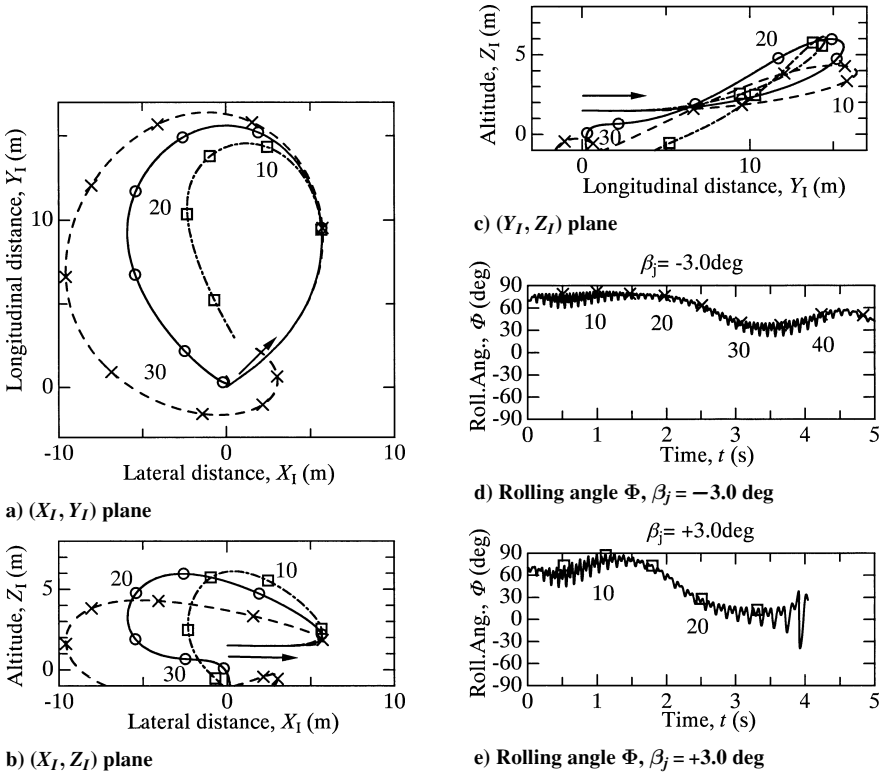

Fig. 9 Effect of the coning angle β_j on the excursion; $U_0 = 25$ m/s, $r_0 = 10$ Hz, and $\Phi_0 = 70$ deg: –×–, $\beta_0 = -3.0$ deg; —○—, $\beta_0 = 0$ deg; and – -□- –, $\beta_0 = +3.0$ deg.

Coning Angle

When the coning angle is increased from $\beta_j = -3$ through $\beta_j = 0$ to $\beta_j = +3$ deg, the excursion radius tends to decrease, as shown in Fig. 9a. The boomerang with the higher coning angle, $\beta_j = +3$ deg, climbs initially and, then, falls and smashes into the ground at about the 26th revolution as can be seen from Figs. 9b and 9c. The first steep climbing and the initial reduction of the bank angle Φ (Figs. 9b, 9c, and 9e) are produced by a very large upward aerodynamic force and pitch-up moment generated by the positive coning angle at high flying speed. The pitch-up moment results from a higher angle of attack when the blade is in the first (forward) half of the rotation, where the apparent disk also has the higher angle of attack and vice versa in the latter (backward) half. This steep climbing causes a large inflow to pass through the rotational plane and leads to the following steep descent and quick reduction of spin rate shown in Fig. 10f. In the short-period oscillation, as seen from Figs. 10a, 10b, 10d, and 10e, no remarkable difference can be found between positive and negative coning angles.

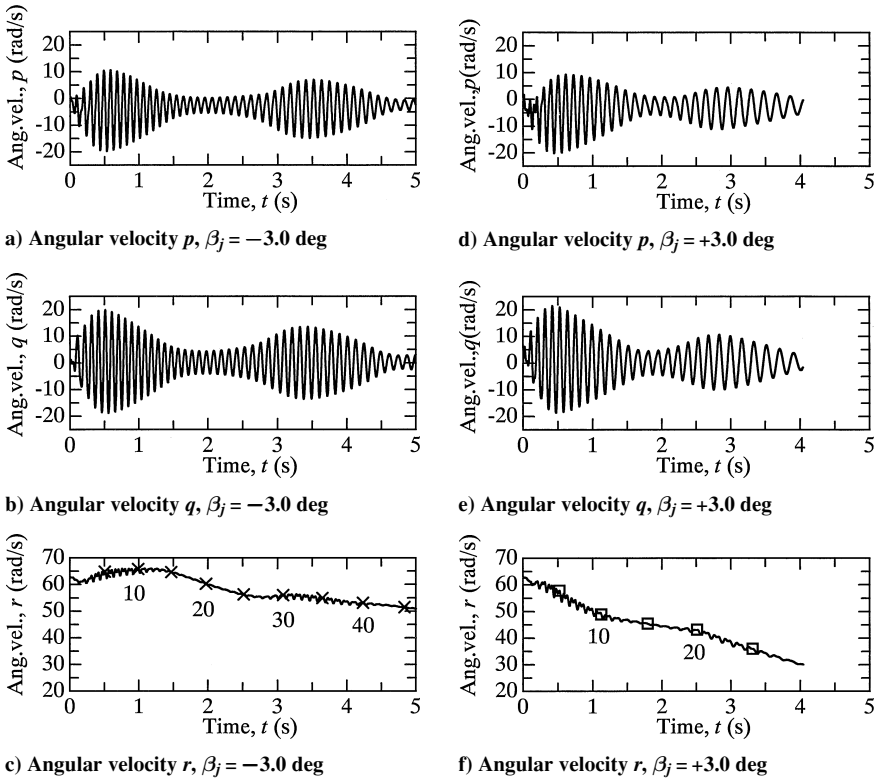

Fig. 10 Time history of angular velocity of coning angle $\beta_j = -3.0$ and +3.0 deg; $U_0 = 25$ m/s, $r_0 = 10$ Hz, and $\Phi_0 = 70$ deg.

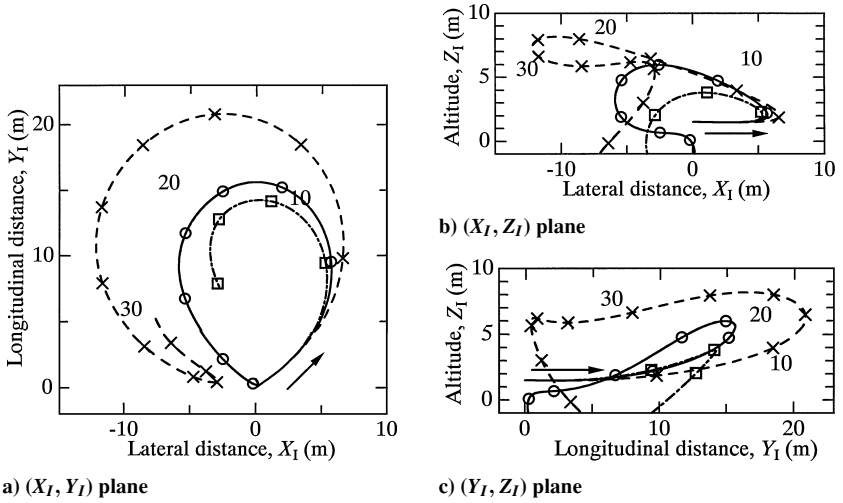

Fig. 11 Effect of the joint angle γ on the excursion; $U_0 = 25$ m/s, $r_0 = 10$ Hz, and $\Phi_0 = 70$ deg: –×–, $\gamma = 130$ deg; —○—, $\gamma = 120$ deg; and – -□- –, $\gamma = 110$ deg.

The negative coning angle, on the other hand, results in an enduring flight accompanied by smaller rolling motion than that of the positive coning angle. Thus, unlike the spin rate of the positive coning angle shown in Fig. 10f, the spin rate is kept close to the initial value (Fig. 10c).

Folding or Joint Angle

The folding angle or joint angle of the reference boomerang was set at $\gamma = 120$ deg or $\Lambda_1 = 120$, $\Lambda_2 = 240$, and $\Delta\Lambda = 60$ deg. When two other folding angles such as $\gamma = 130$ and 110 are selected, the effects of changing the folding angle specifically on the flight stability can be investigated.

In the case of a larger joint angle $\gamma = 130$ deg, turning radius and maximum height increase appreciably, as shown in Figs. 11 and 12. In the theoretical calculation, the boomerang having larger (smaller) moment of inertia can make a flight with higher (lower) altitude and larger (smaller) turning radius than those of the reference excursion because of having higher (lower) tip speed, larger (smaller) angular momentum, and a bit more (less) energy than those of the reference boomerang. However, as stated later, in the flight test of $\gamma = 130$ deg, the boomerang could not fly because of slow spin rate at the takeoff. As shown in Fig. 12, when the joint angle is reduced, the spin rate decreases markedly, and the boomerang lands before reaching the takeoff point.

Tennis Racket Effect

Let us take note of the restoring moment for feathering motion or inertial moment about the y axis. The most effective contribution

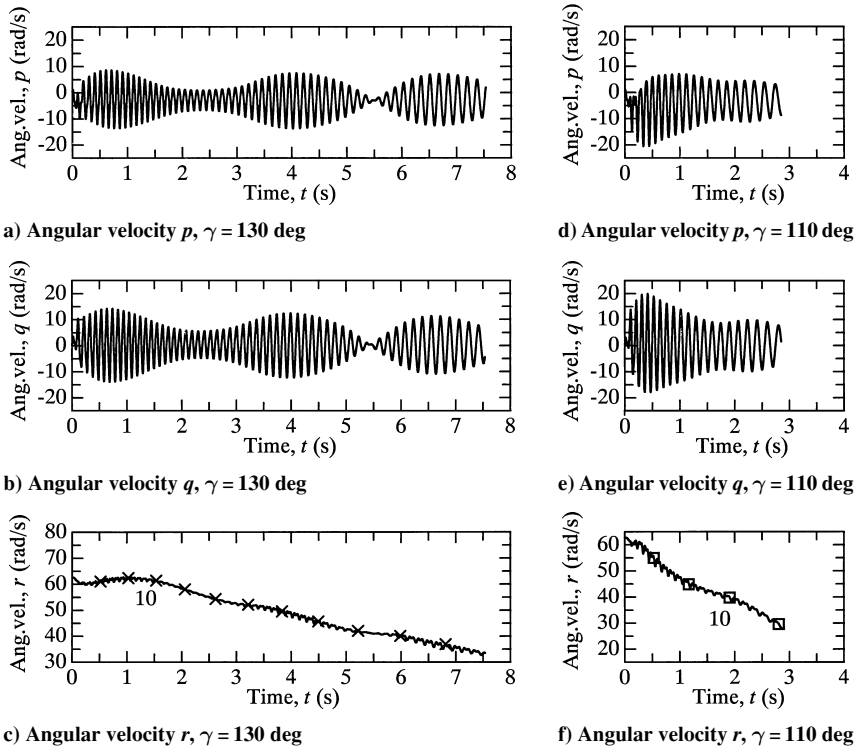

a) Angular velocity p, $\gamma = 130$ deg

b) Angular velocity q, $\gamma = 130$ deg

c) Angular velocity r, $\gamma = 130$ deg

d) Angular velocity p, $\gamma = 110$ deg

e) Angular velocity q, $\gamma = 110$ deg

f) Angular velocity r, $\gamma = 110$ deg

Fig. 12 Effect of the joint angle γ on the angular velocity; $U_0 = 25$ m/s, $r_0 = 10$ Hz, and $\Phi_0 = 70$ deg.

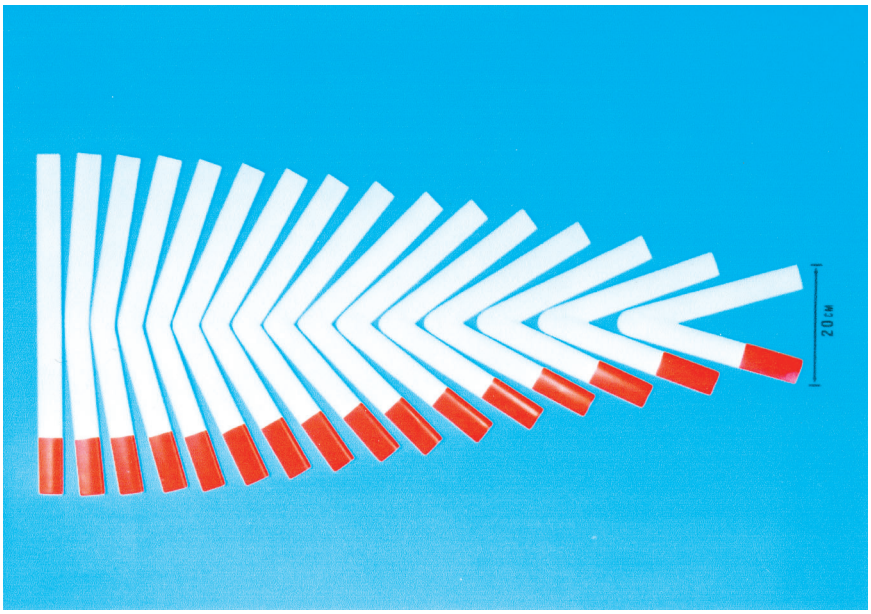

Fig. 13 Various configurations used for the throwing test.

to this restoring moment is made by the centrifugal force $\Delta M_y^I = (I_x - I_y)pr \cong (I_x - I_z)\dot{\psi}^2\theta$. For simplicity of the analysis, let us introduce the following assumptions: 1) The number of blades is two, $n = 2$. 2) Both blades have the same geometrical configuration. 3) The wing cross section is symmetric and homogeneous along the span. 4) Blades do not have coning angle, pitch angle, and twist $\beta_j = \theta_j = \Delta\theta_{t,j} = 0$. 5) The flapping or rolling motion is not considered ($\phi = \dot{\phi} = 0$). 6) The sweep angles Λ_j are given by a folding angle, or a joint angle of two blades γ and a differential angle of $\Delta\Lambda$, such that $\Lambda_1 = \pi/2 + \Delta\Lambda/2 = \pi - \gamma/2$, $\Lambda_2 = 3\pi/2 - \Delta\Lambda/2 = \pi + \gamma/2$, and $\gamma = \Lambda_2 - \Lambda_1 = \pi - \Delta\Lambda$. Then, the restoring moment can be written as

$$\Delta M_y^I = \left\lfloor \left(I_\xi - \tfrac{1}{2}m\bar{\eta}^2\right)\sin^2(\Delta\Lambda/2) + I_\eta \cos^2(\Delta\Lambda/2) - \tfrac{1}{2}m\{c/4\cos(\Delta\Lambda/2)\}^2 \right\rfloor \dot{\psi}^2 \sin(2\theta) \quad (1)$$

where I_ξ, I_η, and $m/2$ are, respectively, the moments of inertia and the blade mass of the respective blades and subscript j has been discarded because of the same geometrical configuration.

Equation (1) can be interpreted as follows: 1) For a straight boomerang ($\Delta\Lambda = 0$), the restoring moment is obtained from the moment of inertia along the feathering axis given by $\{I_\eta - \frac{1}{2}m(c/4)^2\}$ times the centripetal acceleration $\dot{\psi}^2 \sin(2\theta)$, and thus, the wide blade or low-aspect-ratio blade is, like a flying disk, more stable than a slender blade. This inertial contribution to the

restoring moment, derived from the centrifugal force acting on a thin plate (like a tennis racket or a helicopter rotor blade) is called the tennis racket effect. 2) For a folded boomerang ($\gamma < \pi$ or $\Delta\Lambda > 0$), because the contribution of the first term $(I_\xi - \frac{1}{2}m\bar{\eta}^2)\sin^2(\Delta\Lambda/2)$, increases, the restoring moment becomes larger as the folded angle $\Delta\Lambda$ increases due to the larger moment of inertia along the y axis than that of a straight boomerang. These effects are very important for the stability of a boomerang as will be stated later.

Experimental Tests

To determine the flyable range of the folding angle, various boomerangs with different folding angles ($\gamma = 30$–180 deg), whose configurations and dimensions are shown in Fig. 13 and Table 1, respectively, were tested by throwing them at various initial speeds and spin rates.

As shown in Table 2, it was found that the flyable ranges were limited within the joint angle of $40 < \gamma < 120$ deg. Boomerangs with joint angles of either $\gamma < 40$ or $120 < \gamma < 180$ deg were found to be hardly flyable.

In the case of $\gamma = 130$ deg, the calculation shows that the boomerang is flyable at this joint angle, but the experiment shows hardly flyable. The calculation was carried out for the initial spin rate of $r_0 = 10$ Hz. However, it was impossible to get the initial spin rate of the $r_0 = 10$ Hz by the human's throw because of the large moment of inertia.

Table 1 Geometrical configuration of experimental boomerangs

Number	Folding angle γ, deg	Mass, g	Position of c.g. ℓ_c, mm
1	180	77.1	0.0
2	170	76.8	11.0
3	160	74.8	26.0
4	150	84.0	37.5
5	140	87.0	48.5
6	130	94.0	61.0
7	120	85.8	71.5
8	110	81.9	82.5
9	100	97.3	96.0
10	90	80.6	102.0
11	80	74.5	113.0
12	70	73.5	121.0
13	60	87.1	123.5
14	50	80.1	134.0
15	40	79.7	140.0
16	30	84.3	146.5

Conclusions

Boomerang flight dynamics were analyzed theoretically by solving nonlinear equations of motion numerically for a typical returning boomerang as a reference. Then, by changing the initial conditions of throwing, the following results were obtained:

1) When the initial departure speed was reduced (or increased) from that of the reference ($U_0 = 2.5$ m/s), the excursion took a place with a smaller (or larger) radius of curvature than that of the reference excursion.

2) When the initial rolling angle was reduced (or increased) from the reference angle ($\Phi = 75$ deg), the maximum distance of excursion was shorter (or longer) and the altitude of the flight was higher (or lower) than that of the reference.

3) When thrown with very small rolling angle ($\Phi = 0$ deg), the boomerang descended steeply and plummeted to the ground with a potentially damaging impact.

4) When the initial spin rate was reduced (or increased) from that of the reference ($r_0 = 10$ Hz), the turning radius became small (or large) and the amplitude of the short-period oscillation increased (or decreased) appreciably in descending flight.

Changing the geometrical configuration had the following effects on flight performance:

1) When the blade pitch angle was increased (or decreased) from that of the reference angle ($\theta_j = 0$ deg), the turning radius, the maximum distance, the maximum altitude, the duration of flight, and the amplitude of short-period oscillation all decreased (or increased).

2) When the coning angle was increased ($\beta_j = +3$ deg) from that of the reference, the excursion radius decreased and the boomerang smashed into the ground in a shorter flight time. When the coning angle was decreased ($\beta_j = -3$ deg), the boomerang maintained lasting flight accompanied by smaller rolling motion than when the coning angle was positive.

3) When the joint angle was increased (or decreased) from that of the reference, the turning radius and the maximum altitude increased (or decreased) appreciably, but the reduction of the spin rate was very (or not so) marked. For a large joint angle, a higher spin rate is required to return the boomerang.

The preceding conclusions were verified by experimental tests.

Reference

[1]Azuma, A., Beppu, G., Ishikawa, H., and Yasuda, K., "Flight Dynamics of the Boomerang, Part 1: Fundamental Analysis," *Journal of Guidance, Control, and Dynamics*, Vol. 27, No. 4, 2004, pp. 545–554.

Table 2 Flying results of 10 trial flights

Number	Joint angle	1	2	3	4	5	6	7	8	9	10
1	180	×[a]	×	×	×	×	×	×	×	×	×
2	170	×	×	×	×	×	×	×	×	×	×
3	160	×	×	×	×	×	×	×	×	×	×
4	150	×	×	×	×	×	×	×	×	×	×
5	140	×	×	×	×	×	×	×	×	×	×
6	130	×	×	×	×	×	×	×	×	×	×
7	120	◎[b]	◎	×	◎	○[c]	◎	◎	○	○	◎
8	110	○	◎	◎	◎	◎	○	◎	○	○	◎
9	100	◎	×	◎	◎	◎	◎	◎	◎	◎	○
10	90	◎	×	○	○	○	◎	◎	◎	○	×
11	80	○	○	○	○	○	○	○	◎	×	○
12	70	◎	×	◎	◎	×	◎	○	○	◎	◎
13	60	○	◎	○	○	◎	◎	◎	◎	◎	×
14	50	◎	◎	◎	×	——[d]	——	——	——	——	——
15	40	○	◎	◎	○	◎	◎	◎	◎	◎	◎
16	30	×	×	×	×	×	×	×	×	×	×

[a]Unflyable. [b]Flight with one complete circle. [c]Flyable. [d]Damaged.